A 2D interactive spin ladder system, δ´-(BEDT-TTF)$_2$ClC$_2$H$_4$SO$_3$·H$_2$O

Hiroki Akutsu,[†,*] Scott S. Turner,[¶] and Yasuhiro Nakazawa[†]

[†]Department of Chemistry, Graduate School of Science, Osaka University, 1-1 Machikaneyama, Toyokana, Osaka 560-0043, Japan.
[¶]*Department of Chemistry, University of Surrey,* Guildford, Surrey GU2 7XH, U.K.

ABSTRACT: A Curie-Weiss-type paramagnetic δ-(BEDT-TTF)$_2$ClC$_2$H$_4$SO$_3$·H$_2$O with $\theta/2 = j$ = -45.4 K has a phase transition at 160 K, below which the salt has a δ′-type 2D donor arrangement with 1D Heisenberg antiferromagnetic behavior with j = -121.6 K. Further cooling below 140 K induces a weak dimerization in the donor layers leading to a spin ladder system.

Over the past half century, a wide variety of molecular conductors have been prepared.[1] In particular BEDT-TTF-based salts have been found to exhibit most of the collective electronic ground states known to condensed matter (BEDT-TTF = bis(ethylenedithio)tetrathiafulvalene). Typically, the conducting layers consist of BEDT-TTF^{n+} cations, whose molecular arrangements, with chemical pressure caused by the interleaved anions, lead to their physical properties. Theirs transports properties range from insulators to superconductors. For the insulators and semiconductors, the charge carriers cannot freely move and are localized on the donor layers, providing various magnetic ground states. The range of ground states include antiferromagnetic[2] and canted ferromagnetic orderings,[3] spin density wave,[4] 1D and 2D Heisenberg magnets[5] and compounds characterized by a singlet-triplet model,[6] etc. The magnetic moment is not localized in an atomic orbital, as in transition-metal magnets, and not localized in a specific part of a molecule, as in organic radicals but is delocalized across a whole BEDT-TTF molecule. Consequently, the magnetic orbitals overlap directly with each other, which often affords strong magnetic interactions. Moreover, reducing electron correlations by applying pressure or hole and/or electron doping can induce the carriers to become itinerant.

After the report of the first organic conducting salt with an organic sulfonate, (BEDT-TTF)$_2$(*p*-CH$_3$C$_6$H$_4$SO$_3$), by Peter Day's group,[7] sulfonates were widely used as counterions of organic conductors.[8] Accordingly, we have recently reported several charge-transfer (CT) salts of HOC$_2$H$_4$SO$_3^-$ [9] and BrC$_2$H$_4$SO$_3^-$.[10] In this communication, we report a BEDT-TTF-based purely organic semiconducting 2D interactive spin ladder system, δ′-(BEDT-TTF)$_2$ClC$_2$H$_4$SO$_3$·H$_2$O (**1**). Typically, spin ladders are isolated from each other by non-magnetic species,[11] but here the spin ladders interact with each other, hence the term "interactive". Besides the fundamental physical aspects related with spin ladder systems' quantum and topological effects and simple application of switching devices,[11] the interest in spin ladder materials has also been motivated the theoretical prediction that on hole doping they can show superconductivity due to spin mediated hole-hole attraction[12] and pressure-induced superconductivity.[13]

Black rhombus-shaped crystals were obtained by the constant-current electrocrystallization method in 18 mL of CH_2Cl_2 with 10 mg of BEDT-TTF, 44 mg of ClC$_2$H$_4$SO$_3$Na and 67 mg of 18-crown-6 ether. The electrical resistivity was measured by a conventional four-probe method using a HUSO-994C1 multi-channel 4-terminal conductometer. Figure 1 and S1 show ρ *vs.* T and Arrhenius (log ρ *vs.* $1/T$) plots, respectively. The sample shows semiconducting behavior over the investigated temperature. Discontinuities were consistently observed for two measured samples at 165 and 170 K for the cooling and heating processes, respectively. The narrow 5 K width of the hysteresis suggests that it is a 1st order phase transition. The room temperature resistivities of two samples, A and B, are 29.9 and 34.8 Ω·cm, respectively. The activation energies of both samples from 270-290 K (average of the cooling and heating processes) are 0.220 and 0.225 eV, respectively, which are relatively large for BEDT-TTF$^{0.5+}$ salts. However, the gradients of the Arrhenius plots (Figure S1) (= E_a) decrease rapidly with lowering temperature and become constant below the transition, at 0.102 and 0.090 eV for A and B, respectively.

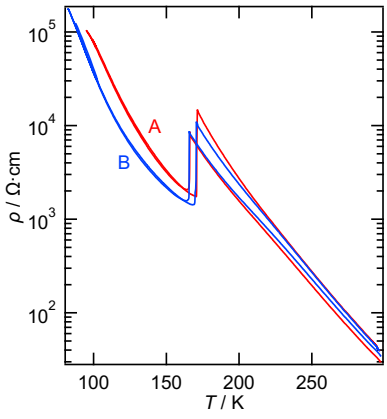

Figure 1. Electrical resistivity of samples A (red) and B (blue) of compound **1**.

X-ray analyses at several temperatures were performed on a Rigaku XtaLAB Synergy Custom with MicroMax-007 HF/VariMax rotating-anode X-ray generator and confocal mono-chromated Mo*K*α radiation. The crystallographic data are shown in Table S1. The structural phase transition was observed between 150 and 160 K for both cooling and heating processes. The small disparity in the

transition temperatures, compared to those found from resistivity measurements, appears to be caused by the different cooling rates. Structures at 290 and 160 K are almost the same. The composition of the high temperature phase is δ-(BEDT-TTF)$_2$ClC$_2$H$_4$Cl·H$_2$O (**1H**). One BEDT-TTF, half an anion and half of a water molecule are crystallographically independent. The crystal structure of **1H** at 290 K is shown in Figure 2a and S2.

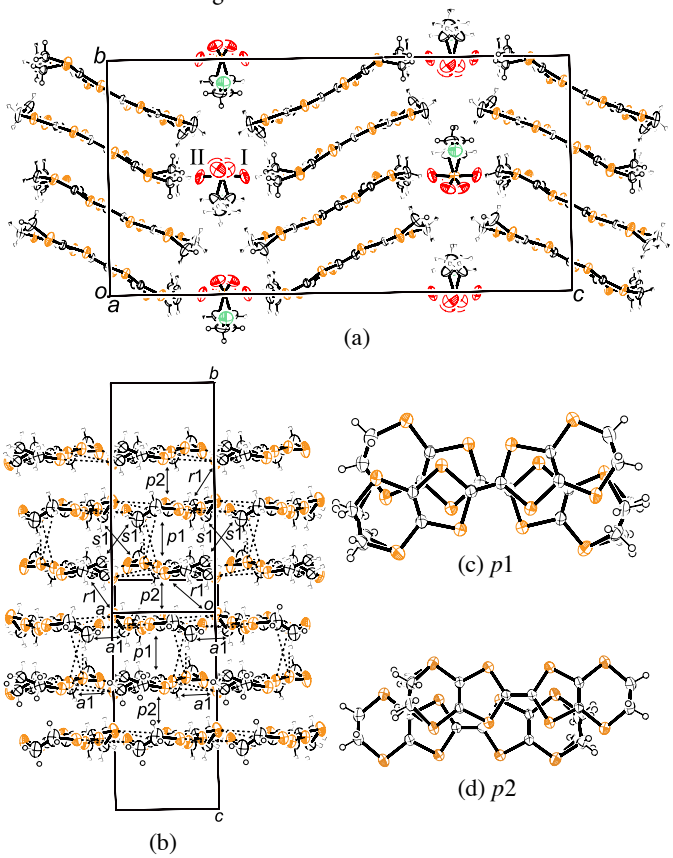

Figure 2. Crystal Structure (a), donor arrangement (b) and two independent overlapping modes (c and d) in the BEDT-TTF stack of **1H** at 290 K.

There are 2D donor layers with many short S···S contacts (Figure 2b), which are interleaved by anion/water layers (Figure 2a and S2). The Cl and S atoms of the anion are located on the mirror plane and are not disordered. The other atoms are not located on the mirror plane and are therefore disordered, since there are two anions having different conformations (I and II), which are superimposed at the same position. Only one of the three oxygen atoms (O3) of -SO_3^- protrudes marginally out of the mirror plane along the *c* and -*c* directions for I and II, respectively. The O3 atom has a contact shorter than the S···O van der Waals distance with S7 of the BEDT-TTF molecule of 3.114(7) Å. In addition, the other oxygen atoms (O1 and O2) form hydrogen bonds with the incorporated water molecules, which are also located on the same mirror plane and not disordered. The packing arrangement in the BEDT-TTF layer is shown in Figure 2b. There are two independent overlapping modes along the stacking direction (//*b*). Overlap *p*1 involves BEDT-TTF molecules that are twisted relative to each other (Figure 2c) and overlap *p*2 involves aligned molecules (Figure 2d). This donor arrangement is termed as δ-type, which typically has metal-insulator (MI) transitions. Furthermore, in δ-salts the transition temperature (T_{MI}) has been found to be proportional to the (cell length along the donor's side-by-side direction)/(cell length along the stacking direction) (*c*/*a* in ref. 7). This ratio for **1H** is 0.41, from which a T_{MI} of 1,300 K is estimated. This suggests that **1H** would be an insulator at room temperature. In fact **1H** is a semiconductor although band calculations[14] reveal Fermi surfaces (Figure S4). Most δ-type salts also show satellite spots or diffuse streaks on the X-ray photos below T_{MI}, resulting from a doubling of the unit cell length along the BEDT-TTF side-by-side direction ($2k_F$-CDW), providing insulating nonmagnetic spin dimer states.[15] However, **1H** has no satellite spots or diffuse streaks at 290, 160 (Figure S6), 140 (Figure S7) and 102 K (Figure S8). This suggests the formation of $4k_F$-CDW in **1H** as discussed below.

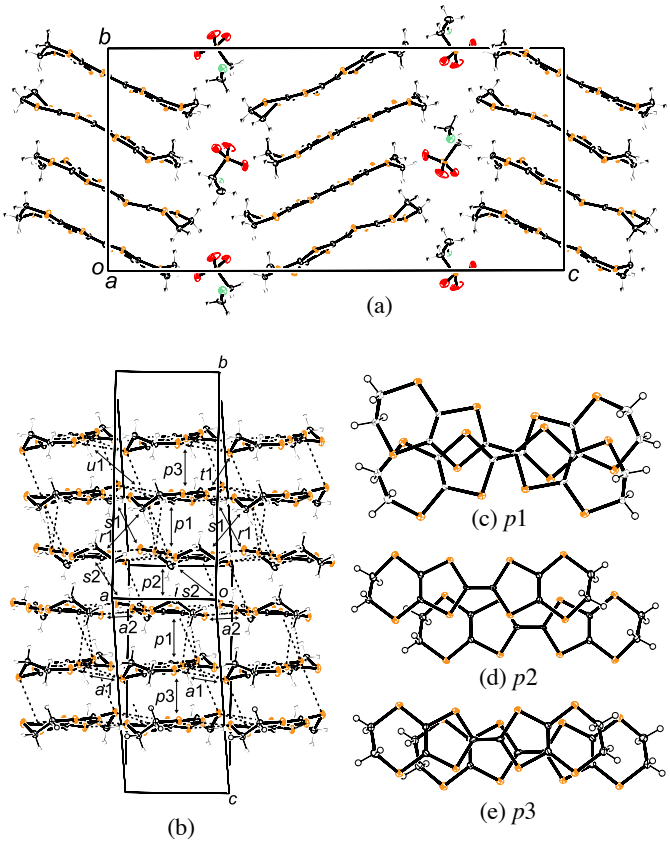

Figure 3. Crystal Structure (a), donor arrangement (b) and three independent overlapping modes (c, d and e) in the BEDT-TTF stack of **1L** at 102 K.

Below the phase transition, the cell parameters change as shown in Table S1. The composition of the low temperature phase is found to be δ′-(BEDT-TTF)$_2$ClC$_2$H$_4$Cl·H$_2$O (**1L**). The cell parameters at 150, 140, 120, and 102 K are almost the same (Table S1); the crystal structure of **1L** at 102 K is shown in Figure 3a and S3. The Laue group (space group) changes from orthorhombic (*Pbcm*) for **1H** to monoclinic ($P2_1/c$) for **1L**. The low temperature phase (**1L**) has two donors, one anion and one water molecule in the asymmetric unit and one crystallographically independent donor stack in the unit cell. The independent anion is located on a general position and is ordered, indicating that the phase transition coincides with the order-disorder transition of the anion. Figure S9 shows the temperature dependence of the cell volume of **1**. On cooling a sharp decrease in the cell volume of approximately 50 Å^3 occurs around 160 K. The cell volume shrinks by approximately 1.5 % at the order-disorder transition suggesting that the disorder of the anion above 160 K is

dynamic. During the phase transition, the donor packing motif also changes from δ to δ′.[15] The δ and δ′ donor arrangements, shown in Figure 2b and 3b, are quite similar, although going from **1H** to **1L** the number of the independent donor molecules increases to 2, and the number of overlap modes increases to 3. The *p*3 overlap mode in **1L** (Figure 3e) is significantly different from both the *p*1 and p2 modes in **1**H (Figure 2c and 2d) and **1L** (Figure 3c and 3d). Therefore, in **1L** each donor forms in a tetramer, suggesting that **1L** is a band insulator. Indeed, the calculated band electronic structure,[14] shown in Figure S5, has no Fermi surfaces. However, the band gap is more than five times smaller than the Mott gap as shown in Table S2, suggesting that spin localization appears to be more stable than spin dimerization.

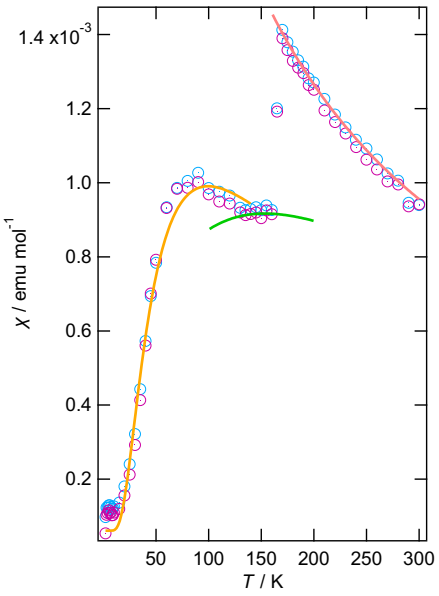

Figure 4. Magnetic susceptibility of **1**. Pale blue and pink circles indicate cooling and heating plots, respectively. Red, green and orange solid lines are calculated on the basis of a Curie-Weiss, 1D Heisenberg and Spin ladder model, respectively.

The temperature-dependent magnetic susceptibility of **1** was measured using a Quantum Design MSMS-2S SQUID magnetometer from 2-300 K. There is a large susceptibility drop at 160 K as shown in Figure 4, at which the magnetic interaction (j) changes drastically such that **1L** has larger j than **1H**. As mentioned above, at the phase transition cell volume shrinkage was also observed. The data in the high temperature range can be fitted to a Curie-Weiss law (red solid curve in Figure 4) with C = 0.352 emu mol^{-1} K^{-1} and θ = -90.8 K ($j = \theta/2$ = -45.4 K).‡ It is relevant to note that α′-type BEDT-TTF-based salts, the donor layers of which consist of only twisted stacks, are 1D Heisenberg magnets, where the 1D chain extends along the BEDT-TTF side-by-side direction.[16] The 1D magnetic chain of **1L** also appears to extend along the side-by-side direction. The θ value is smaller than the phase transition temperature so that no significant deviation of the magnetic susceptibility from the Curie-Weiss curve (red solid curve in Figure 4) is observed. Below the phase transition, the data can be fitted to a 1D Heisenberg model (Eq. S1) with j = -121.6 K (green solid curve in Figure 4). Although it was not possible to estimate the Curie constant because of the narrow temperature range and fixed value of C = 0.375 emu mol^{-1} K^{-1} that was used during the curve fitting. The j value of the green curve is almost three times larger than that of the red curve, which explains the discontinuity in the susceptibility. The cell volume shrinkage appears to make the donor-donor interaction stronger. If the salt is a normal 1D Heisenberg magnet, a susceptibility drop caused by a spin Peierls transition is usually observed and the system goes into a non-magnetic ground state. In contrast, the salt shows a different and unique behavior. The magnetic susceptibility shows an upturn around 140 K, has a broad peak at 100 K and then decreases monotonically down to base temperature. The susceptibility curve cannot be fitted by a Singlet-Triplet model, which we previously reported for another δ′-type salt[6b] but can be fitted to a spin ladder model (eq. 1) with C = 0.375 emu mol^{-1} K^{-1} (fixed), a = 1.90 K and Δ = 100 K.[‡, 11, 17, 18]

$$\chi = \frac{2C}{\sqrt{\pi\left(\frac{a}{k_B}\right)T}} e^{-\Delta/k_B T} \qquad (1)$$

In fact, high symmetrical **1H** has only two overlap modes (p1 and p2) such that only a 1D spin chain can exist but a spin ladder cannot be formed. This is schematically shown in Figure 5 (left), where p1 is stronger than p2, therefore each dimer related by the p1 overlap has a spin. By contrast, the lower symmetrical **1L** has three overlap modes (p1, p2 and p3), and a spin ladder can be formed if magnetic interaction of p2 is not equal to p3 as shown in Figure 5 (right). In addition, the largest interlayer transfer integral of 2.2 × 10^{-6} was calculated, suggesting that the interlayer interaction J_{inter} is approx. 10^{-7} times smaller than those of intralayer interaction.

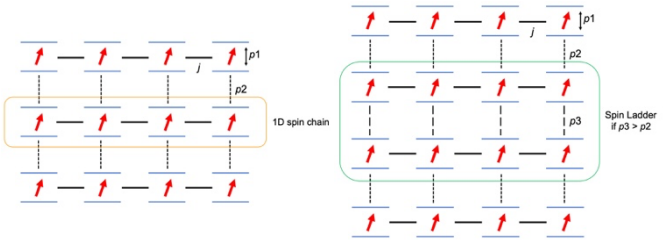

Figure 5. Schematic diagrams of spin structures of a 1D chain of **1H** (left) and a spin ladder of **1L** (right).

Several spin ladder systems of organic charge transfer salts have been reported,[11,17] in which each ladder is isolated by insulating counterions. Therefore, their inter-ladder interactions are very weak. In contrast, the inter-ladder interaction of **1L** is strong by virtue of many S···S contacts between the ladders. Moreover, the magnetic susceptibility of **1L** from 140 to 160 K obeys a 1D Heisenberg model where the difference between p2 and p3 is negligible. This implies that the ratio of p2 to p3 deviates from 1.0 when the system acts as a spin ladder. Figure 6 shows a plot of $p2/p3$ versus T. The p2/p3 ratio decreases with decreasing temperature, and no anomalies are observed at 140 K. Thus it is not a phase transition and a critical value of $p2/p3$, below which the susceptibility of the system obeys a spin ladder system, is approximately 0.9. Since magnetic interactions j_2 and j_3 (along the p2 and p3 overlaps, respectively) are proportional to the roots of the overlap integrals, the critical value of j_2/j_3 of approximately 0.8 is evaluated. In addition, since the 1D Heisenberg magnets usually show spin Peierls transition, dimerisation is observed along the chain direction in salt **1** (side-by-side direction). However, the 1D chains of salt **1** interact with each other along the interchain direction (along the stacking direction), the 2D interaction likely prevents the spin Peierls transition. The strategy is similar

to that used in $(TMTSF)_2X$ salts (TMTSF = tetraselenafulvalene and X = monoanion),[4] in which significant Se···Se side-by-side interactions prevent the Peierls transition, and superconductivity is shown at high pressure. In addition, the magnetic topology of **1L** is still unclear for only performing the band structure calculations. Another more precise calculation and/or existence of plateau on a magnetization curve are needed for conformation of spin ladder system.

Finally, we roughly estimate j, j_2 and j_3 using Eq. 2,[11, 17, 18] where $j' = j_3$. For this estimation, we set $j_2 = 0.8j_3$ and the j value is assumed to be the same as a 1D Heisenberg chain from 140-160 K, j = 120 K.

$$\Delta = j' - j + \frac{1}{2}\frac{j^2}{j'} \qquad (2)$$

The resultant j, j_2 and j_3 of 120, 30, and 40 K, respectively, are estimated.

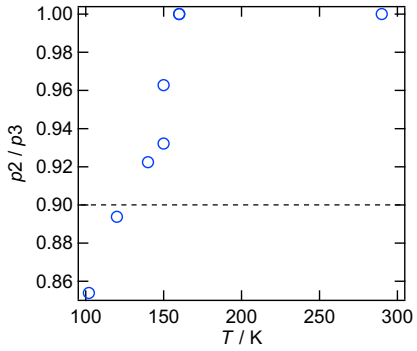

Figure 6. $p2/p3$ versus T plots of **1**. The dashed line is a guide to the eye, showing $p2/p3 = 0.90$.

In conclusions, δ-$(BEDT\text{-}TTF)_2ClC_2H_4SO_3 \cdot H_2O$ is a Mott insulator and shows a Curie-Weiss behaviour ($\theta/2 = j = -45.4$ K). There is a phase transition with a susceptibility jump at 160 K, below which the resultant δ′-$(BEDT\text{-}TTF)_2ClC_2H_4SO_3 \cdot H_2O$ obeys a 1D Heisenberg model down to 140 K. Significant 2D interactions prevent the formation of density waves along the donor layer chain (side-by-side). A weak dimerization along the stacking direction below 140 K occurs, leading to a purely organic 2D interactive spin ladder system.

ASSOCIATED CONTENT

Supporting Information

The Supporting Information is available free of charge on the ACS Publications website.

Temperature-dependent crystallographic data, Arrhenius plots of the resistivities, the results of band structure calculations, and Ewald sphere of **1H** at 160 K.

AUTHOR INFORMATION

Corresponding Author

Hiroki Akutsu – *Department of Chemistry, Graduate School of Science, Osaka University, Machikaneyama, Toyonaka, Osaka 560-0043, Japan*; oricd.org/0000-0002-8350-2246;
Email: akutsu@chem.sci.osaka-u.ac.jp

Author Contributions

The manuscript was written through contributions of all authors. All authors have given approval to the final version of the manuscript.

Notes

‡ We have used a mean field model[10] for the curve fittings to estimate the inter-chain or inter-ladder interactions, however, the changes of the curvatures before and after applying the mean field model are so subtle that we were not able to estimate the interactions.

REFERENCES

(1) (a) Williams, J.M.; Ferraro, J.R.; Thorn, R.J.; Carlson, K.D. ; Geiser, U.; Wang, H.H.; Kini, A.M.; Whangbo M.-H. *Organic Superconductor (Including Fullerenes) Synthesis, Structure, Properties and Theory*; Prentice-Hall: New York, U.S.A, 1992. (b) Mori, T. *Electronic Properties of Organic Conductors*; Springer Japan: Tokyo, Japan, 2016.

(2) (a) Maeda, K.; Hara, T.; Nakamura, T. ESR study on low-dimensional antiferromagnets α-$(BEDT\text{-}TTF)_2PF_6$ and ζ-$(BEDT\text{-}TTF)_2PF_6(THF)$. *Synth. Met.*, **2005**, *152*, 453. (b) Tokumoto, M.; Anzai, H.; Ishiguro, T.; Saito, G.; Kobayashi, H.; Kato, R.; Kobayashi, A. Electrical and magnetic properties of organic semiconductors, $(BEDT\text{-}TTF)_2X$ (X = IBr_2, IBrCl, and ICl_2). *Synth. Met.*, **1987**, *19*, 215-220. (c) Yoneyama, N.; Miyazaki, A.; Enoki, T.; Saito, G. Magnetic properties of $(BEDT\text{-}TTF)_2X$ with localized spins. *Synth. Met.*, **1997**, *86*, 2029-2030.

(3) Welp, U.; Fleshler, S.; Kwok, W. K.; Crabtree, G. W.; Carlson, K. D.; Wang, H. H.; Geiser, U.; Williams, J. M.; Hitsman, V. M. Weak ferromagnetism in κ-$(ET)_2Cu[N(CN)_2]Cl$. *Phisica B*, **1993**, *186-188*, 1065-1067.

(4) Jérome, D. Organic Conductors: From Charge Density Wave TTF–TCNQ to Superconducting $(TMTSF)_2PF_6$. *Chem. Rev.*, **2004**, *104*, 5565-5592.

(5) (a) Akutsu, H.; Ishihara, K.; Ito, S.; Nishiyama, F.; Yamada, J.; Nakatsuji, S.; Turner S. S.; Nakazawa Y. Anion polarity-induced self-doping in a purely organic paramagnetic conductor, α′-α′-$(BEDT\text{-}TTF)_2(PO\text{-}CONH\text{-}m\text{-}C_6H_4SO_3)\cdot H_2O$ where BEDT-TTF is bis(ethylenedithio)tetrathiafulvalene and PO is the radical 2,2,5,5-Tetramethyl-3-pyrrolin-1-oxyl. *Polyhedron*, **2017**, *136*, 23-29. (b) Akutsu, H.; Yamada, J.; Nakatsuji, S.; Turner, S. S. A New BEDT-TTF-Based Organic Charge Transfer Salt with a New Anionic Strong Acceptor, N,N'-Disulfo-1,4-benzoquinonediimine. *Crystals*, **2012**, *2*, 182-192. (c) Akutsu, H.; Yamada, J.; Nakatsuji, S.; Turner, S. S. Structures and properties of a BEDT-TTF-based organic charge transfer salt and the zwitterion of ferrocenesulfonate. *Dalton Trans.*, **2013**, *42*, 16351-16354.

(6) (a) Yamashita, A.; Akutsu, H.; Yamada, J.; Nakatsuji, S.; Turner, S. S. New organic magnetic anions $TEMPO\text{-}CONA(CH_2)_nSO_3^-$ (n = 0–3 for A = H, n = 2 for A = CH_3) and their TTF, TMTSF, and/or BEDT-TTF salts. *Polyhedron*, **2005**, *24*, 2796-2802. (b) Akutsu, H.; Kohno, A.; Turner, S. S.; Nakazawa, Y. Structure and Properties of a New Purely Organic Magnetic Conductor, δ′-$(BEDT\text{-}TTF)_2(PO\text{-}CONHCH(cyclopropyl)SO_3)\cdot 1.7H_2O$. *Chem. Lett.*, **2020**, *49*, 1345-1348.

(7) Chasseau, D.; Watkin, D.; Rosseinsky, M. J.; Kurmoo, M.; Talham, D. R.; Day P. Syntheses, crystal structures and physical properties of conducting salts $(BEDT\text{-}TTF)_2X$ (X = CF_3SO_3 or $p\text{-}CH_3C_6H_4SO_3$). *Synth. Met.* **1988**, *24*, 117-125.

(8) Geiser, U.; Schlueter, J. A. Conducting Organic Radical Cation Salts with Organic and Organometallic Anions. *Chem. Rev.* **2004**, *104*, 5203-5241.

(9) Akutsu, H.; Koyama, Y.; Turner, S.S.; Furuta, K.; Nakazawa, Y. Structures and Properties of New Organic Conductors: BEDT-TTF, BEST and BETS Salts of the $HOC_2H_4SO_3^-$ Anion. *Crystals* **2020**, *10*, 775-1-13.

(10) Akutsu, H.; Koyama, Y.; Turner, S. S.; Nakazawa, Y. Structures and Properties of New Organic Molecule-Based Metals, $(D)_2BrC_2H_4SO_3$ [D = BEDT-TTF and BETS]. *Magnetochem.* **2021**, *7*, 91.

(11) Silva, R. A. L.; Almeida, M. Spin-ladder behaviour in molecular materials. *J. Mater. Chem.*, **2021**, *9*, 10573-10590.

(12) Dagotto, E.; Rice, T. M. Surprises on the Way from One- to Two-Dimensional Quantum Magnets: The Ladder Materials. *Science*, **1996**, *271*, 12-13.
(13) Takahashi., T.; Sugimoto, A.; Manabu, Y.; Yamaguchi, T.; Hirata, Y.; Kawakami, T.; Avdeev, M.; Matsubayashi, K.; Du, F.; Kawashima, C.; Soeda, H.; Nakano, S.; Uwatoko, Y.; Ueda, Y. Sato, T. J.; Ohgushi, K. Pressure-induces superconductivity in the iron-based ladder material $BaFe_2S_3$. *Nature Mat.*, **2015**, *14*, 1008-1013.
(14) Mori, T.; Kobayashi, A.; Sasaki, Y.; Kobayashi, H.; Saito, G.; Inokuchi, H. The Intermolecular Interaction of Tetrathiafulvalene and Bis(ethylenedithio)tetrathiafulvalene in Organic Metals. Calculation of Orbital Overlaps and Models of Energy-band Structures. *Bull. Chem. Soc. Jpn.* **1984**, *57*, 627-633 (The software package is available from http://http://www.op.titech.ac.jp/lab/mori/lib/program.html).
(15) Mori, T. Structural Genealogy of BEDT-TTF-Based Organic Conductors III. Twisted Molecules: δ and α′ Phases. *Bull. Chem. Soc. Jpn.*, **1999**, *72*, 2011-2027.
(16) (a) Obertelli, S. D.; Friend, R. H.; Talham, D. R.; Kurmoo, M.; Day, P. The magnetic susceptibility and EPR of the organic conductors α'-$(BEDT\text{-}TTF)_2X$, X=$AuBr_2$, $CuCl_2$ and $Ag(CN)_2$. *J. Phys.: Condens. Matter*, **1989**, *1*, 5671-5680. (b) Kurmoo, M.; Allan, M.; Friend, R.; Chasseau, D.; Bravic, G.; Day, P. $(BEDT\text{-}TTF)_2GaCl_4$: Structure, electrical and magnetic properties. *Synth. Met.*, **1991**, *42*, 2127-2130. (c) Mallah, T.; Hollis, C.; Bott, S.; Kurmoo, M.; Day, P.; Allan, M.; Friend, R. H. Crystal structures and physical properties of bis(ethylenedithio)-tetrathiafulvalene charge-transfer salts with FeX_4^-(X = Cl or Br) anions. *J. Chem. Soc., Dalton. Trans.*, **1990**, 859-865.
(17) (a) Komatsu, T.; Kojima, N.; Saito, G. Magnetic properties of an organic spin-ladder compound $(BEDT\text{-}TTF)Zn(SCN)_3$. *Solid State Commun.*, **1997**, *103*, 519-523. (b) Imai, H.; Inabe, T.; Otsuka, T.; Okuno, T.; Awaga, K. Molecular spin ladder in the $Ni(dmit)_2$ (dmit=1,3-dithiol-2-thione-4,5-dithiolate) salt with a nitronyl nitroxide cation. *Phys. Rev. B*, **1996**, *54*, R6838-R6840. (c) Rovira, C.; Veciana, J.; Ribera, E.; Tarres, J.; Canadell, E.; Rousseau, R.; Mas, M.; Molins, E.; Almeida, M.; Henriques, R. T.; Morgado, J.; Schoeffel, J. -P.; Pouget, J.- P. An Organic Spin-Ladder Molecular Material. *Angew. Chem., Int. Ed. Engl.* **1997**, *36*, 2324-2326. (d) Ribera, E.; Rovira, C.; Veciana, J.; Tarreś, J.; Canadell, E.; Rousseau, R.; Molins, E.; Mas, M.; Schoeffel, J. -P.; Pouget, J. -P.; Morgado, J.; Henriques, R. T.; Almeida, M. The $[(DT\text{-}TTF)_2M(mnt)_2]$ Family of Radical Ion Salts: From a Spin Ladder to Delocalised Conduction Electrons That Interact with Localised Magnetic Moments. *Chem.–Eur. J.*, **1999**, *5*, 2025. (e) Arcon, D.; Lappas, A.; Margadonna, S.; Prassides, K.; Ribera, E.; Veciana, J.; Rovira, C.; Henriques, R. T.; Almeida, M. Magnetic behavior of a two-leg organic spin-ladder compound. *Phys. Rev. B*, **1999**, *60*, 4191-4194. (f) Silva, R. A. L.; Santos, I. C.; Wright, J.; Coutinho, J. T.; Pereira, L. C. J.; Lopes, E. B.; Rabaça, S.; Vidal-Gancedo, J.; Rovira, C.; Almeida, M.; Belo, D. Dithiophene-TTF Salts; New Ladder Structures and Spin-Ladder Behavior. *Inorg. Chem.*, **2015**, *54*, 7000-7006.
(18) Troyer, M.; Tsunetsugu, H.; Warts, D. Thermodynamics and spin gap of the Heisenberg ladder calculated by the look-ahead Lanczos algorithm. *Phys. Rev. B*, **1994**, *50*, 13515-13527.

For Table of Contents Use Only,

A 2D interactive spin ladder system, δ′-$(BEDT\text{-}TTF)_2ClC_2H_4SO_3{\cdot}H_2O$

Hiroki Akutsu,* Scott S. Turner, and Yasuhiro Nakazawa

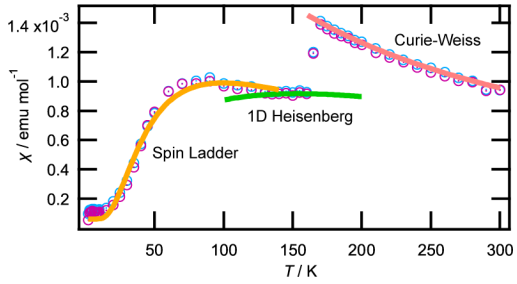

A Curie-Weiss-type paramagnetic δ-$(BEDT\text{-}TTF)_2ClC_2H_4SO_3{\cdot}H_2O$ with $\theta/2 = j$ = -45.4 K has a phase transition at 160 K, below which the salt has a δ′-type 2D donor arrangement with 1D Heisenberg antiferromagnetic behavior with j = -121.6 K. Further cooling below 140 K induces a weak dimerization in the donor layers leading to a spin ladder system.